
Feedback Guidance of Diffusion Models

Felix Koulischer^{1,*} Florian Handke² Johannes Deleu¹
 Thomas Demeester^{1,†} Luca Ambrogioni^{2,†}

¹ Ghent University - imec

² Donders Institute for Brain Cognition and Behaviour, Radboud University

Abstract

While Classifier-Free Guidance (CFG) has become standard for improving sample fidelity in conditional diffusion models, it can harm diversity and induce memorization by applying constant guidance regardless of whether a particular sample needs correction. We propose **FeedBack Guidance** (FBG), which uses a state-dependent coefficient to self-regulate guidance amounts based on need. Our approach is derived from first principles by assuming the learned conditional distribution is linearly corrupted by the unconditional distribution, contrasting with CFG’s implicit multiplicative assumption. Our scheme relies on feedback of its own predictions about the conditional signal informativeness to adapt guidance dynamically during inference, challenging the view of guidance as a fixed hyperparameter. The approach is benchmarked on ImageNet512x512, where it significantly outperforms Classifier-Free Guidance and is competitive to Limited Interval Guidance (LIG) while benefitting from a strong mathematical framework. On Text-To-Image generation, we demonstrate that, as anticipated, our approach automatically applies higher guidance scales for complex prompts than for simpler ones and that it can be easily combined with existing guidance schemes such as CFG or LIG. Our code is available at this link.

1 Introduction

At the heart of the image and video generation revolution led by diffusion models [1–5] lies the conditioning algorithm most well-known as the *guidance* mechanism [6, 7]. The need for diffusion guidance stems from the inherent challenge of learning conditional distributions with limited paired data, which is why further emphasizing the signal using a parameter referred to as the guidance scale proves advantageous in practice [6]. This parameter allows to push the predictions from the conditional model further from those of the unconditional model, essentially reinforcing the difference between them [7, 8]. This is more well-known as the Classifier-Free Guidance (CFG) algorithm [7]. It is only after the introduction of the guidance algorithm, that diffusion models gained the impressive performance they are nowadays known for. Recent works have however made clear that applying guidance on the entire sampling trajectory is not only unnecessary but also harms performance [9, 10]. By applying guidance in the beginning of the generative process, the model tends to converge to specific condition-dependent low frequency details [7, 9, 11], severely reducing the diversity of the generated samples. On the other hand, applying guidance towards the end of the generative process is largely unnecessary as both unconditional and conditional estimates converge, both being equally capable of denoising the high-frequency features [8, 9].

These results can be understood theoretically based on the recently developed theory of spontaneous symmetry breaking phase transitions [12–14]. This theory predicts that so called ‘speciation’ transi-

[†] Joint Senior Authors

^{*} Corresponding author: felix.koulischer@ugent.be

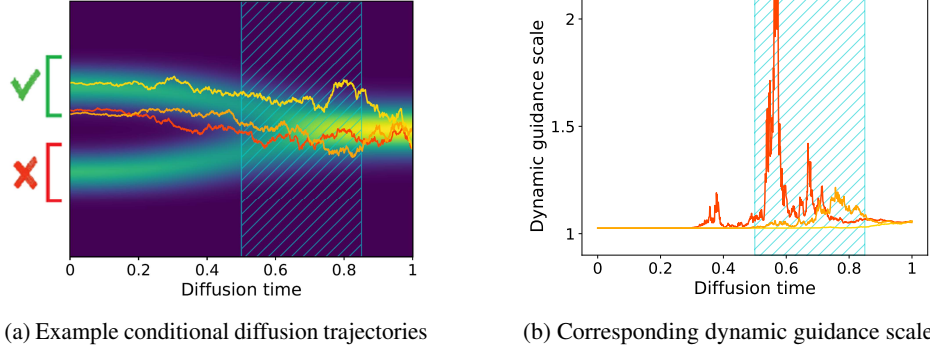


Figure 1: Illustrative diffusion trajectories and their hypothetical guidance scales in a 1D setting. Trajectories located further from the mode close to the decision window receive higher guidance.

tions during generative diffusion correspond to particular ‘decision points’ when some features of the generations, such as for example class identity, are maximally sensitive to guidance [15–17]. Since the timing of these critical windows depends on both the data and the conditioning signal, it is natural to consider dynamic forms of guidance where the guidance scale is determined state-dependently.

In this work, we provide a principled methodology to obtain dynamic guidance formulas. Our scheme relies on feedback of a quality estimation of its current predictions, which is why we refer to our scheme as **FeedBack Guidance (FBG)** in analogy with control theory. As shown in Fig. 1, if a trajectory is estimated as more likely to be originating from the unconditional model than from the conditional model, the guidance scale increases to correct the error and realign the sample towards the correct class. Similarly to the empirically justified work on Limited Interval Guidance (LIG)[9], our self-regulated guidance scale is only present at intermediate noise levels, which now follows from first principles.

2 Preliminaries

To introduce our FeedBack Guidance scheme (FBG), the working principles behind Denoising Diffusion Probabilistic Models (DDPMs) and Classifier-Free-Guidance (CFG) are required. These are summarized in sections 2.1 and 2.2. In section 2.3, an overview of the current stand of literature with respect to diffusion guidance is given.

2.1 Denoising Diffusion Probabilistic Models (DDPM)

Diffusion models [1–5] are progressive denoisers, that aim to invert a forward noising schedule by learning the score function, defined as the gradient of the log-likelihood of the marginals $\nabla_{\mathbf{x}} \log p_t(\mathbf{x}; \theta)$. In the case of Variance Exploding (VE) DDPM, this forward noising process iteratively adds Gaussian noise to a clean data distribution. This way, the underlying data distribution $q(\mathbf{x}, 0)$ is progressively noised until a Gaussian of very large variance is obtained, i.e. until after T steps $q(\mathbf{x}, T) \sim \mathcal{N}(\mathbf{x}; \mathbf{0}, \sigma_T^2 \mathbf{I})$, with $\sigma_T \gg 1$. For any forward noising schedule $\{\sigma_t\}_{t=1}^T$, whereby $\mathbf{x}_{t+1} = \mathbf{x}_t + \sigma_{t+1|t} \epsilon_t$ (with $\epsilon_t \sim \mathcal{N}(\epsilon_t; \mathbf{0}, \mathbf{I})$ and $\sigma_{t+1|t}^2 = \sigma_{t+1}^2 - \sigma_t^2$), the forward process can be directly sampled at any step t , according to $q(\mathbf{x}_t | \mathbf{x}_0) \sim \mathcal{N}(\mathbf{x}_t; \mathbf{x}_0, \sigma_{t|0}^2 \mathbf{I})$, with $\sigma_{t|0}^2 = \sum_{i=0}^{t-1} \sigma_{i+1|i}^2 = \sigma_t^2$. The goal is to learn a score based model, that is able to iteratively reverse this forward process. This backward process can be decomposed into a Markov chain

$$p(\mathbf{x}_{t:T}; \theta) = p(\mathbf{x}_T) \prod_{i=t+1}^T p_i(\mathbf{x}_{i-1} | \mathbf{x}_i; \theta) \quad (1)$$

Crucially, each step of the Markov chain is by construction approximately Gaussian $p_t(\mathbf{x}_{t-1} | \mathbf{x}_t; \theta) \sim \mathcal{N}(\mathbf{x}_{t-1}; \boldsymbol{\mu}_{t-1}(\mathbf{x}_t), \sigma_{t-1|t}^2 \mathbf{I})$ with $\sigma_{t-1|t}^2 = \sigma_{t-1}^2 (1 - \frac{\sigma_{t-1}^2}{\sigma_t^2})$. Instead of modeling the mean, $\boldsymbol{\mu}_{t-1}$, it is common to train a denoiser that predicts the final denoised output at any diffusion stage

$\hat{\mathbf{x}}_{0|t} = \mathbb{E}_{q(\mathbf{x}_0|\mathbf{x}_t)}(\mathbf{x}_0)$ ¹. In the case of a VE-scheduler, the two are connected by the following identity:

$$\boldsymbol{\mu}_{\theta,t-1} = \frac{\sigma_{t-1}^2}{\sigma_t^2} \mathbf{x}_t - \left(1 - \frac{\sigma_{t-1}^2}{\sigma_t^2}\right) \hat{\mathbf{x}}_{0|t} \quad (2)$$

It should also be noted that the sought after score function is proportional to the learned denoiser.

2.2 Classifier-Free Guidance

Learning a highly complex conditional distribution, such as that required for Text-To-Image (T2I), is a challenging task. In most situations it is only possible to poorly approximate this target distribution, which can be seen from the vague predictions generated by sampling a "pure" conditionally trained diffusion model, such as the one present in Stable diffusion [18]. To amplify the conditioning signal present during the denoising process, diverse solutions exist. The most widely used method is that of diffusion guidance, of which the simplest example is that of Classifier (-Free) Guidance [6, 7]. The guidance mechanism is used in all variants of diffusion, from Flow Matching [19, 20] to Discrete Diffusion Models [21]. The reasoning behind guidance is to sharpen the marginals towards the posterior likelihood $p_{\theta,t}(c|\mathbf{x}_t)$ using an exponent λ referred to as the guidance scale, i.e. to consider a λ -sharpened conditional marginal distribution $\tilde{p}_t(\mathbf{x}_t|c) = p_{\theta,t}(\mathbf{x}_t)p_{\theta,t}(c|\mathbf{x}_t)^\lambda$. When λ is equal to one this reduces to sampling the conditional model, while setting $\lambda > 1$ further sharpens the marginals towards regions that better satisfy the condition c . To obtain a Classifier-Free scheme, independent of the posterior $p_{\theta,t}(c|\mathbf{x}_t)$, it suffices to rewrite the posterior probability as a ratio of the conditional and unconditional likelihoods $p_{\theta,t}(c|\mathbf{x}_t) \propto p_{\theta,t}(\mathbf{x}_t|c)/p_{\theta,t}(\mathbf{x}_t)$. From a score-based perspective this results in the well known guidance equation:

$$\begin{aligned} \nabla \log \tilde{p}_t(\mathbf{x}_t|c) &= \nabla \log p_{\theta,t}(\mathbf{x}_t) + \lambda \nabla \log p_{\theta,t}(c|\mathbf{x}_t) \\ &= \nabla \log p_{\theta,t}(\mathbf{x}_t) + \lambda (\nabla \log p_{\theta,t}(\mathbf{x}_t|c) - \nabla \log p_{\theta,t}(\mathbf{x}_t)) \end{aligned} \quad (3)$$

In the first formulation the gradient of a classifier appears, if this likelihood is directly parametrised using pretrained networks one obtains what is referred to as training-free guidance [6, 22]. The main challenge of these approaches is that they leverage a model trained solely on clean samples to offer guidance on noisy samples [22, 23]. The second equation is that of Classifier-Free Guidance [7], which has as main inconvenience that it requires joint conditional-unconditional model training [5, 7, 18, 24].

2.3 Related Work

Conditional generation, and in particular the topic of guidance, is a very active research field. As this paper is centered around Classifier-Free Guidance and its derivatives in the context of Diffusion Models, this section will provide a concise exploration of the field's key developments, with readers seeking comprehensive context directed to existing in-depth survey literature [25, 26]. A prominent research direction preserves the core framework of CFG while introducing various predefined time-varying profiles to replace the rigid constant guidance scale [9, 10, 27, 28]. Noteworthy in this regard, due to its computational advantage, simplicity and its effectiveness, is choosing a limited interval in which guidance should be applied [9]. Precisely where this limited interval is located depends on the underlying quality of the conditional model. The better the model, as is the case for the EDM2 models on which that particular paper focuses, the later the guidance can be activated. Interestingly different intervals are found when evaluating performance using the FID[29] or $\text{FD}_{\text{DinoV2}}$ [30], the latter being much wider and earlier.

Less researched is the approach of a state-dependent guidance scale, which has been shown to be theoretically optimal in the context of negative guidance [31, 32], but has only been heuristically proposed for positive guidance [33, 34]. Our work is the first to derive a state- and time-dependent guidance scale from first principles.

Another recent breakthrough is that of autoguidance, which highlights that instead of pushing away from an expensive qualitative unconditional model it is advantageous to move away from a far less performant conditional model [8]. The latter could for instance be a smaller model of a same model-family [8], but it could also be a model which is not trained until convergence [8, 35], or even a model falsely conditioned at earlier timesteps [36]. The idea of these approaches is that when using

¹Equivalently, the noise $\hat{\boldsymbol{\epsilon}}_t$ can be predicted, the two are connected by the identity $\mathbf{x}_t = \hat{\mathbf{x}}_{0|t} + \sigma_t \hat{\boldsymbol{\epsilon}}_t$

guidance one should not only emphasize the class specific details (by reinforcing along the difference of the conditional and unconditional models) but also the details that make the image high quality (by reinforcing along the difference of a highly qualitative model and of a far less qualitative model). Key for this is that the errors of the smaller model are similar in nature to those of the larger one, only bigger [8, 35, 36]. Our Feedback scheme can be easily adapted to obtain equations entirely compatible with these ideas.

A newly emerging research direction, has proposed to step away from guidance as a whole and instead perform a tree-search over a limited amount of trajectories and selectively choose the most promising ones using reward models [37, 38]. These approaches are still very recent, but might lead to an entire different era of conditional diffusion generation, in which instead of relying on guidance, the model has the ability to focus on the most promising trajectories to obtain the most of the learned models. Our feedback approach, and in particular the posterior estimation algorithm, could potentially provide a meaningful way of ranking these paths using solely the pretrained diffusion models.

3 Feedback Guidance

This section presents the theoretical foundation of Feedback Guidance. In section 3.1, we introduce a framework that reformulates guidance formulas as the result of assumptions about systematic errors in the learned distributions. In section 3.2 we demonstrate that adopting an additive rather than multiplicative error assumption naturally produces a dynamic guidance mechanism that adapts throughout the generation process. The resulting state- and time-dependent guidance scale requires posterior likelihood estimation, achieved by monitoring the Markov chain, outlined in section 3.3. In section 3.4 the key hyperparameters of FBG are discussed.

3.1 Interpreting guidance schemes through error assumptions

Here, we conceptualize guidance formulas as the result of inverting an error model that determines how the unconditional distribution ‘corrupts’ the estimated conditional distribution. This form of corruption is to be expected since the model is far less frequently trained on a given class or prompt, which implies that a large part of the training signal is unconditional. In the case of CFG, by reversing Eq. (3) and substituting $\gamma = 1/\lambda$ it becomes clear that CFG implicitly assumes that the learned conditional distribution, denoted by the subscript θ in this work $p_{\theta,t}(\mathbf{x}_t|c)$, is a multiplicative mixture of the true conditional and unconditional distributions:

$$\begin{aligned} p_{\theta,t}(\mathbf{x}_t|c) &\propto p_t(\mathbf{x}_t)^{\frac{1-\lambda}{\lambda}} p_t(\mathbf{x}_t|c)^{\frac{1}{\lambda}} \\ &= p_t(\mathbf{x}_t)^{\gamma-1} p_t(\mathbf{x}_t|c)^{\gamma} \end{aligned} \quad (4)$$

In the case when $\gamma \approx 1$ (low guidance regime), the modelled conditional corresponds to the true conditional. In that setting, sampling the learned conditional is sufficient. However, when $\gamma \approx 0$ (strong guidance regime), the modelled conditional resembles the *unconditional* distribution, which is precisely why strong guidance is required during sampling.

3.2 Feedback Guidance

In control theory jargon, both standard CFG and LIG are examples of open-loop controllers since the guidance scale is not a function of the current state \mathbf{x}_t . This means that the guidance formula will

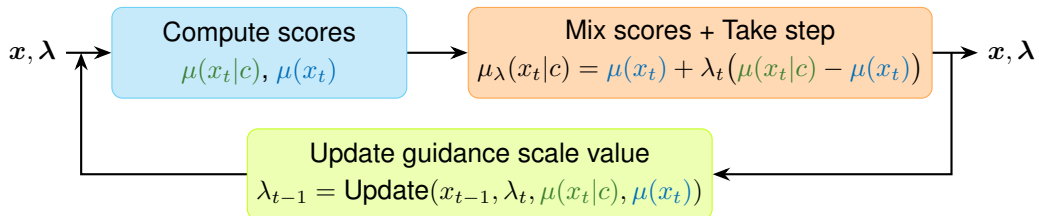


Figure 2: Schematic of Feedback guidance (FBG). The state space consists of both \mathbf{x}_t and λ , which are updated iteratively during the denoising process. The guidance scale is updated by tracking the posterior ratio thanks to Eq. (11), which can then be inserted in Eq. (8).

equally affect all states, regardless of their quality and class alignment. We argue that might lead to over-saturation and stereotypical generations in situations where the conditional model is already good enough to be sampled on its own, as is the case for simplistic or memorized prompts.

Here, we derive a guidance formula that implements a form of feedback, or closed-loop control. From an error perspective we assume that the learned conditional distribution corresponds to an additive mixture of the true conditional and unconditional distributions:

$$p_{\theta,t}(\mathbf{x}_t|c) = (1 - \pi)p_t(\mathbf{x}_t) + \pi p_t(\mathbf{x}_t|c) \quad (5)$$

The additive assumption is arguably more realistic since in contrast to the multiplicative assumption, it gives non-zero probability mass to regions lying outside the conditional c . A direct benefit of the additive mixture assumption is that it commutes with the forward diffusion kernel. This implies that defining an estimated additive error on the denoised distribution corresponds to assuming the same error on the marginals. This is often mistakenly assumed in the context of the multiplicative mixture considered in CFG, which is discussed in more detail in Appendix A.

Assuming a well-modeled unconditional distribution, i.e. $p_{\theta,t}(\mathbf{x}_t) \approx p_t(\mathbf{x}_t)$, this implies sampling:

$$p(\mathbf{x}_t|c) \propto p_{\theta,t}(\mathbf{x}_t|c) - (1 - \pi)p_{\theta,t}(\mathbf{x}_t) \quad (6)$$

In other words, we propose removing a portion of the unconditional distribution from the modeled conditional before sampling. This, similarly to the approach taken in CFG, helps strengthen the conditioning signal, as regions that do not satisfy c are pushed towards zero-likelihood.

Of key interest for sampling is the score function of the underlying conditional distribution $\nabla_{\mathbf{x}} \log p(\mathbf{x}|c)$, which can be derived using the chain rule:

$$\nabla_{\mathbf{x}} \log p(\mathbf{x}_t|c) = \nabla_{\mathbf{x}} \log p_{\theta,t}(\mathbf{x}_t) + \lambda(\mathbf{x}_t, t) \left(\nabla_{\mathbf{x}} \log p_{\theta,t}(\mathbf{x}_t|c) - \nabla_{\mathbf{x}_t} \log p_{\theta,t}(\mathbf{x}_t) \right), \quad (7)$$

with as guidance scale

$$\lambda(\mathbf{x}_t, t) = \frac{p_{\theta,t}(c|\mathbf{x}_t)/p_{\theta,t}(c)}{p_{\theta,t}(c|\mathbf{x}_t)/p_{\theta,t}(c) - (1 - \pi)}. \quad (8)$$

The additive error model results in a state- and time-dependent guidance scale that can be expressed in terms of the posterior likelihood $p_{\theta,t}(c|\mathbf{x}_t)$. The guidance scale is equal to one when the posterior likelihood is high, and exhibits an asymptotic behavior as the posterior approaches $1 - \pi$. The mixing parameter π determines when guidance is deemed necessary: if π is close to one, indicating a well learned distribution, guidance is only activated when $p_{\theta,t}(c|\mathbf{x}_t)$ reaches very low values. In contrast, for poorly learned distributions, with smaller values of π , guidance is easily activated as soon as the posterior decreases. It should be noted that if $0 < p_{\theta,t}(c|\mathbf{x}_t) < 1 - \pi$ the guidance scale is negative. We argue that in the continuous case this situation would never arise since the guidance scale would need to cross the asymptote, which should in turn increase the posterior. To avoid this happening in the discretized case, we clamp the posterior to a minimum value p_{\min} , which in practice implies clamping the guidance scale at λ_{\max}^2 .

In practice, our dynamic guidance scale defined by Eq. (8) can easily be added on top of any pre-existing guidance method such as CFG or LIG. To make it clear which methods are used, we introduce the following notation: FBG_{pure} corresponds to using solely Eq. (8) as guidance scale, FBG_{CFG} corresponds to adding some base classifier-free guidance on top and FBG_{LIG} corresponds to adding some base guidance in a limited interval only. We refer to FBG as all approaches that use variants of Eq. (8) for guidance. The corresponding error models assumed for these schemes are given in Appendix D.1.

3.3 Posterior approximation by tracking the Markov Chain

Our novel dynamic guidance scale $\lambda(\mathbf{x}, t)$ relies on the posterior likelihood $p_{\theta,t}(c|\mathbf{x})$, which is in general not available using score-based models. Leveraging recent ideas by from [31], we approximate the required posterior $p(c|\mathbf{x}_t)$ by estimating the required likelihoods by tracking the diffusion Markov Chain, defined by Eq. (1) during the denoising process. The key of this posterior approximation is that the likelihood ratio between the conditional and unconditional models can be updated iteratively as follows:

$$\log p_{\theta,t}(c|\mathbf{x}_{t:T}) = \log p_{\theta,t+1}(c|\mathbf{x}_{t+1:T}) + \log p_{\theta,t}(\mathbf{x}_t|\mathbf{x}_{t+1}, c) - \log p_{\theta,t}(\mathbf{x}_t|\mathbf{x}_{t+1}) \quad (9)$$

²The two are connected by the identity $p_{\min} = \log \left((1 - \pi) \frac{\lambda_{\max}}{\lambda_{\max} - 1} \right)$, for more details see Appendix B.2

Guidance scheme	FID (\downarrow)		FD _{DinoV2} (\downarrow)		Prec. (\uparrow)		Rec. (\uparrow)	
	Stoch.	PFODE	Stoch.	PFODE	Stoch.	PFODE	Stoch.	PFODE
CFG	5.00	2.97	100.2	88.4	0.85	0.84	0.73	0.75
LIG	3.59	2.31	88.5	77.1	0.86	0.86	0.75	0.77
FBG _{pure} (ours)	3.76	2.50	89.0	75.6	0.86	0.86	0.76	0.77
FBG _{LIG} (ours)	3.62	2.45	87.9	74.6	0.87	0.86	0.75	0.76

Table 1: Evaluation of different guidance methods using EDM2-XS using a stochastic and a 2nd-order Heun sampler. FID and FD_{DinoV2} values refer to the model optimized under the respective metrics, FD_{DinoV2}. Precision and Recall are computed on 10240 samples with 5 nearest neighbour with models optimized under FD_{DinoV2} [30, 41].

The complex non-linear interplay between the three hyperparameters of our approach $-\pi$, τ , and δ makes it challenging to predict how changing one parameter affects the overall guidance profile. To address this issue, we propose a more intuitive parameterization that allows users to directly control the characteristics of the guidance profile through normalized diffusion timesteps. Instead of directly tuning τ and δ , we express them as functions of two more interpretable parameters: t_0 and t_1 . Here, t_0 represents the normalized diffusion time at which the guidance scale reaches a predefined reference value λ_{ref} (set to 3 without loss of generality), while t_1 represents an estimant of the normalized diffusion time at which the guidance reaches its maximum value³.

4 Results

The novel state-dependent dynamic guidance scheme is validated in the context of image generation on Imagenet512x512 using the EDM2-XS model. Our guidance scheme largely outperforms CFG and is competitive with LIG while benefitting from a strong mathematical framework. In the context of T2I, multiple qualitative examples are provided in combination with results illustrating that the self-regulated feedback guidance scale increases on average with the difficulty of the prompt.

4.1 Comparison of Guidance Schemes on Class Conditional Generation

For our class-conditional experiments, we utilize the EDM2-XS model [8, 24] trained on ImageNet512x512 [42] using 64 function evaluations. We evaluate performance using multiple metrics: FID [29], FD_{DinoV2} [30], as well as Precision and Recall [41]. The latter two provide comprehensive insights into the quality-diversity trade-off exhibited by different guidance approaches [9, 30, 41]. In alignment with our theoretical framework for posterior estimation—which is based on Markov chain sampling—we primarily focus on stochastic sampling methods. However, we note that our approach demonstrates comparable effectiveness when following the probability flow ODE, which we implement using a 2nd-order Heun sampler [5, 24].

The baselines comparisons are optimized for the chosen samplers. With CFG [7], a grid search to determine the optimal guidance scale is performed at decimal resolution. For LIG [9], we follow the recommendations and first perform a joint grid search over both the noise level σ_{max} at which the guidance is activated and the guidance scale at decimal resolution and thereafter optimize the ending point of guidance at σ_{min} ⁴. The optimal hyperparameters can be found in Table 2. Notably, we find that the optimal parameter values vary not only based on the metric being optimized (FID or FD_{DinoV2}) but also differ significantly between samplers. For our Feedback Guidance approach, parameter sweeps over t_0 and $t_0 - t_1$ across multiple values of π are performed. Notably, the offset parameter δ depends on both t_0 and π , which significantly reduces the sensitivity of our approach to variations in the mixture coefficient π .

To visualize the effects of these parameters, we present FD_{DinoV2} sweeps as a heatmap in Fig. 3 (a corresponding FID heatmap is provided in Appendix D). The optimized hyperparameter values are detailed in Table 2 in Appendix D, with performance metrics summarized in Table 1. Consistent with findings for LIG, we observe that optimal FD_{DinoV2} performance requires guidance to be activated

³The mathematical details are provided and explained in Appendix B.2

⁴In contrast to the remarks made in [9], we find that guidance during the later stages of diffusion is not only unnecessary but actually harmful, especially when looking at the FD_{DinoV2}.

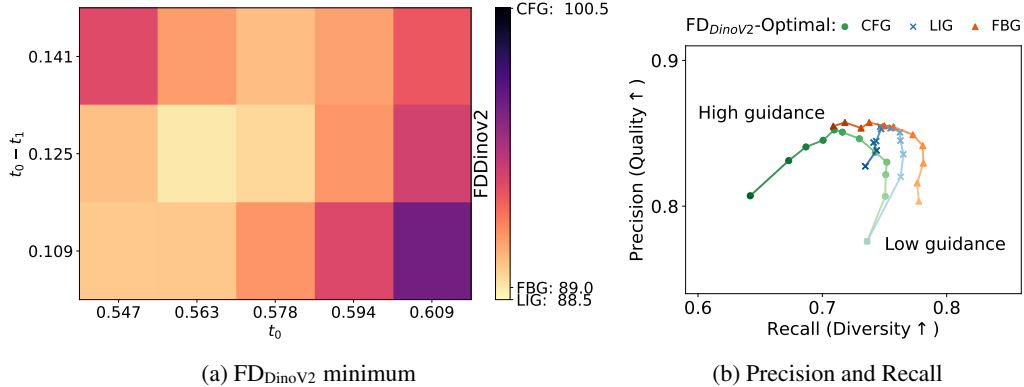


Figure 3: In (a) the grid search over the two hyperparameters t_0 and t_1 . The FD_{DinoV2} is shown calibrated within the best performing value between CFG, LIG and FBG. In (b) precision and recall sweeps at FD_{DinoV2} optimum of each approach. For LIG and CFG a sweep over the guidance scale at fixed interval is performed, while for FBG a sweep over t_0 at fixed $t_0 - t_1$ is performed. The amount of guidance applied is visualised through the color intensity.

earlier and maintained longer than for optimal FID, corresponding to higher values of both t_0 and $t_0 - t_1$. Our results demonstrate that pure Feedback Guidance outperforms CFG on both FD_{DinoV2} and FID metrics, while remaining competitive with LIG across these measurements. To analyze the quality-diversity trade-off, Precision and Recall curves on 10,240 images using a 5-nearest neighbor approach, with optimal FD_{DinoV2} hyperparameters are computed. For CFG and LIG, the sweep is performed across guidance scales ranging from 1 to 4. Since FBG_{pure} lacks a directly comparable hyperparameter, a sweep over t_0 while maintaining a fixed interval $t_0 - t_1 = 0.125$ corresponding to 8/64 steps is instead performed. These analyses illustrate the inherent trade-off between image quality and diversity when applying guidance techniques. While CFG struggles to improve quality without substantially compromising diversity, LIG preserves diversity more effectively—likely because its narrow, late-stage guidance interval minimally affects the low-frequency components of generated images. In contrast, FBG achieves a wide Recall range comparable to CFG but with a significantly better Precision trade-off, representing an advantageous balance between quality and diversity.

In addition, we optimize our FBG_{LIG} scheme, which can be seen as a combination of FBG_{pure} and LIG, as described at the end of section 3.2. For simplicity the separately optimized interval is kept for LIG and solely the guidance scale is altered, while both π and t_0 are kept the same as the optimal values found in FBG_{pure} and solely t_1 is altered. We do not exclude the possibility that a full grid search might yield better results. This guidance scheme outperforms its parts when measured using the FD_{DinoV2} ⁵, illustrating the complementarity of the approaches.

4.2 Guidance on Text-To-Image

In the context of Text-To-Image (T2I), our approach is evaluated using Stable diffusion 2 [18], for which a VE-scheduler is implemented [5, 24]. To remain consistent with the theory a stochastic sampler is used using 32 function evaluations. The purpose of this section is not to investigate to what extent Feedback Guidance may outperform CFG or LIG in terms of image quality, but merely to demonstrate the promise of the approach.

On its own, the conditional model used in T2I applications is of far lower quality than is the case for the EDM2 models, which is precisely why in practice much larger guidance scales are required [7, 18]. For FBG this implies that π has to be chosen much smaller, all results in this section use a value of $\pi = 0.85$ in combination with $t_0 = 0.75$ and $t_1 = 0.5$. In practice, we also find it helpful to remove the offset from the posterior approximation towards the end of the generative process⁶. We find that using a limited amount of CFG with $\lambda_{CFG} = 1.5$ can help to retrieve low frequency features

⁵The FD_{DinoV2} has been shown to correlate much more with human perception than the typically used FID[30].

⁶To be specific in this context we choose $\delta = 0$ if $t < 0.3$.

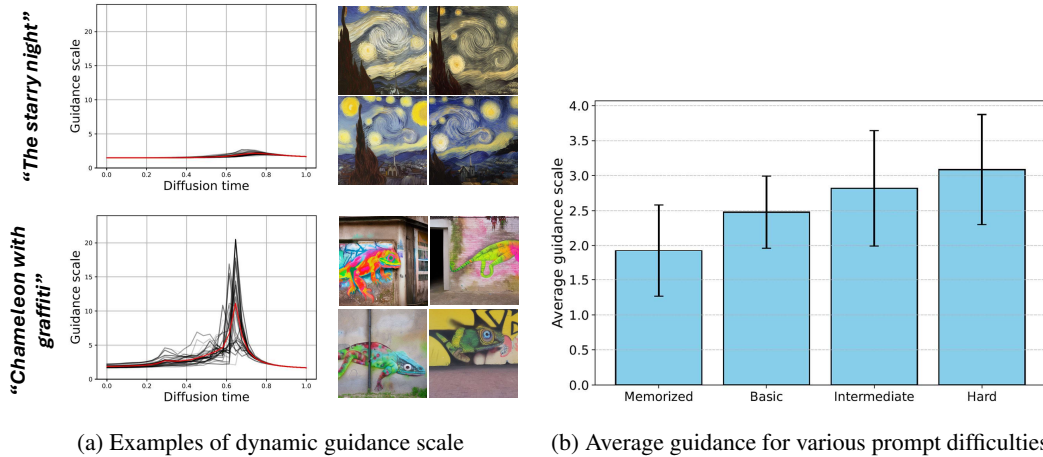


Figure 4: Analysis of FBG in the context of T2I. In (a) the dynamic guidance scale of 32 samples are shown using two prompts: a memorized one ("The starry night by Van Gogh") and a more difficult one ("A chameleon blending into a graffiti-covered wall"). For both a base level of CFG is added with $\lambda = 1.5$. In (b) the average guidance scale applied when using FBG is shown as a function of various prompt difficulties. The prompts are specified in Appendix E.

such as sharp colors, without significantly harming diversity, which is why in this context we propose to use FBG_{CFG} . All illustrative samples shown are generated using the latter.

Prompt specificity of FBG: One of the main advantages of Feedback Guidance is that the denoising process of different prompts are allowed to behave differently. This is in stark contrast with current guidance approaches that apply a fixed profile to every prompt for any trajectory regardless of the complexity of the prompt. We argue that well-learned prompts such as for instance "The starry night" which is likely to be memorized by the network should receive minimal amounts of guidance. On the contrary, complex prompts containing detailed descriptions should receive much stronger levels of guidance to be accurately reproduced. To analyse whether such a phenomenon is observed, we design a small prompt dataset containing 60 prompts of 4 difficulty levels: memorized, easy, intermediate and very hard⁷. The average guidance scale obtained using FBG is then averaged over 32 samples per prompt for these four categories. As shown in Fig.4b, Feedback Guidance is, as expected, most present in situations where the prompt is difficult to model.

Trajectory specificity of FBG: Another key property of FBG is its state, or trajectory, dependence. For the same prompt, two trajectories might receive entirely different levels of guidance. This is illustrated in Fig. 5: if the conditional model is, by chance, already close to the desired result, a minimal amount of guidance is applied, whereas if the conditional model is far off guidance is much more present.

5 Limitations and Future Work

Our FBG approach opens several new directions in the theory and practice of guidance. The adopted additive mixture model was chosen based on its mathematical simplicity, but it is likely not a close approximation of the true systematic biases in trained models. More precise error models could potentially be obtained by studying the training dynamics of the models and tracking the relative error of conditional and unconditional scores, which may lead to more accurate dynamic guidance formulas. Similarly, our choice of prior is solely based on simplicity, and other options should be investigated both theoretically and empirically. Finally, due to computational constraints, our evaluation currently focuses on EDM2-XS models. Future work should explore the method’s performance characteristics on larger architectures such as EDM2-L, as well as conduct quantitative analysis of the Text-To-Image case.

⁷For more details on the dataset, we refer the reader to appendix E

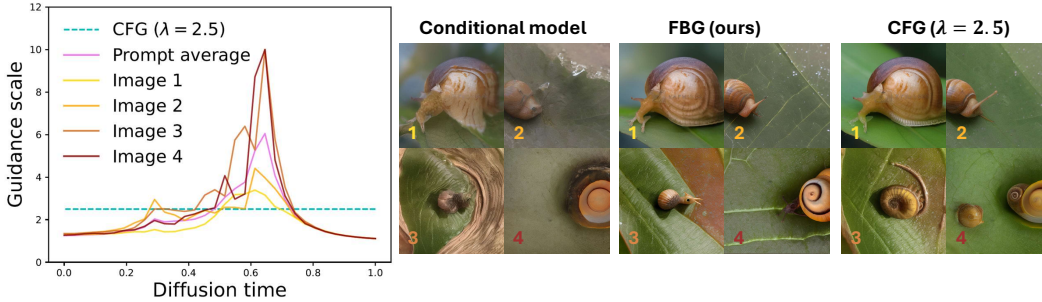


Figure 5: Guidance scale for different trajectories using the prompt: “A snail crawling on a green leaf with water droplets”. If the conditional prediction is good the guidance is low (top two images). In contrast when the conditional prediction is poor, the guidance scale increases (bottom two images).

6 Conclusion

In this work, we introduced a novel view of the commonly used guidance mechanism, interpreting guidance as a way of rectifying the errors made by the learned conditional model. By replacing the implicitly assumed multiplicative error of Classifier-Free Guidance (CFG) with an additive one, we obtained Feedback Guidance (FBG)—a state- and time-dependent guidance mechanism that dynamically relies on the model’s own prediction to estimate how much guidance is needed during inference. This work challenges the view of guidance as a fixed global scheme and instead allows different trajectories and conditions to behave differently. Our results demonstrate that FBG significantly outperforms CFG, and is competitive with Limited Interval Guidance (LIG) while relying on solid theoretical grounds.

Acknowledgments

This research was partly funded by the Research Foundation - Flanders (FWO-Vlaanderen) under grant G0C2723N and by the Flemish Government (AI Research Program).

References

- [1] Jascha Sohl-Dickstein et al. “Deep Unsupervised Learning using Nonequilibrium Thermodynamics”. In: *Proceedings of the 32nd International Conference on Machine Learning*. Vol. 37. 2015. URL: <https://proceedings.mlr.press/v37/sohl-dickstein15.html>.
- [2] Jonathan Ho, Ajay Jain, and Pieter Abbeel. “Denoising Diffusion Probabilistic Models”. In: *Advances in Neural Information Processing Systems*. Vol. 33. 2020. URL: https://proceedings.neurips.cc/paper_files/paper/2020/file/4c5bcfec8584af0d967f1ab10179ca4b-Paper.pdf.
- [3] Jiaming Song, Chenlin Meng, and Stefano Ermon. “Denoising Diffusion Implicit Models”. In: *International Conference on Learning Representations*. 2021. URL: <https://openreview.net/forum?id=St1giarCHLP>.
- [4] Yang Song et al. “Maximum Likelihood Training of Score-Based Diffusion Models”. In: *Advances in Neural Information Processing Systems*. Ed. by M. Ranzato et al. Vol. 34. 2021. URL: https://proceedings.neurips.cc/paper_files/paper/2021/file/0a9fddb17feb6ccb7ec405cfb85222c4-Paper.pdf.
- [5] Tero Karras et al. “Elucidating the Design Space of Diffusion-Based Generative Models”. In: *Advances in Neural Information Processing Systems*. Vol. 35. 2022, pp. 26565–26577. URL: https://proceedings.neurips.cc/paper_files/paper/2022/file/a98846e9d9cc01cfb87eb694d946ce6b-Paper-Conference.pdf.
- [6] Prafulla Dhariwal and Alexander Nichol. “Diffusion Models Beat GANs on Image Synthesis”. In: *Advances in Neural Information Processing Systems*. Vol. 34. 2021. URL: https://proceedings.neurips.cc/paper_files/paper/2021/file/49ad23d1ec9fa4bd8d77d02681df5cfa-Paper.pdf.

- [7] Jonathan Ho and Tim Salimans. “Classifier-Free Diffusion Guidance”. In: *NeurIPS 2021 Workshop on Deep Generative Models and Downstream Applications*. 2021. URL: <https://openreview.net/forum?id=qw8AKxfYbI>.
- [8] Tero Karras et al. “Guiding a Diffusion Model with a Bad Version of Itself”. In: *Advances in Neural Information Processing Systems*. Vol. 37. 2024. URL: https://proceedings.neurips.cc/paper_files/paper/2024/file/5ee7ed60a7e8169012224dec5fe0d27f-Paper-Conference.pdf.
- [9] Tuomas Kynkäänniemi et al. “Applying Guidance in a Limited Interval Improves Sample and Distribution Quality in Diffusion Models”. In: *The Thirty-eighth Annual Conference on Neural Information Processing Systems*. 2024. URL: <https://openreview.net/forum?id=nAIhvNy15T>.
- [10] Seyedmorteza Sadat et al. “CADS: Unleashing the Diversity of Diffusion Models through Condition-Annealed Sampling”. In: *The Twelfth International Conference on Learning Representations*. 2024. URL: <https://openreview.net/forum?id=zMoNraj2X>.
- [11] Sander Dieleman. “Diffusion is spectral autoregression”. In: *Blog post* (2024). URL: <https://sander.ai/2024/09/02/spectral-autoregression.html>.
- [12] Gabriel Raya and Luca Ambrogioni. “Spontaneous symmetry breaking in generative diffusion models”. In: *Thirty-seventh Conference on Neural Information Processing Systems*. 2023. URL: <https://openreview.net/forum?id=lxGFGMMSV1>.
- [13] Antonio Sclocchi, Alessandro Favero, and Matthieu Wyart. “A Phase Transition in Diffusion Models Reveals the Hierarchical Nature of Data”. In: *arXiv preprint arXiv:2402.16991* (2024).
- [14] Luca Ambrogioni. “The Statistical Thermodynamics of Generative Diffusion Models: Phase Transitions, Symmetry Breaking, and Critical Instability”. In: *Entropy* 27 (2025). URL: <https://www.mdpi.com/1099-4300/27/3/291>.
- [15] Giulio Biroli et al. “Dynamical regimes of diffusion models”. In: *Nature Communications* (2024). URL: <https://doi.org/10.1038/s41467-024-54281-3>.
- [16] Marvin Li and Sitan Chen. “Critical windows: non-asymptotic theory for feature emergence in diffusion models”. In: *arXiv preprint arXiv:2403.01633* (2024).
- [17] Florian Handke et al. “Measuring Semantic Information Production in Generative Diffusion Models”. In: *ICLR 2025 Workshop on Deep Generative Model in Machine Learning: Theory, Principle and Efficacy*. 2025. URL: <https://openreview.net/forum?id=QDRK34bWUC>.
- [18] R. Rombach et al. “High-Resolution Image Synthesis with Latent Diffusion Models”. In: *2022 IEEE/CVF Conference on Computer Vision and Pattern Recognition (CVPR)*. 2022. URL: <https://doi.ieeecomputersociety.org/10.1109/CVPR52688.2022.01042>.
- [19] Yaron Lipman et al. “Flow Matching for Generative Modeling”. In: *The Eleventh International Conference on Learning Representations*. 2023. URL: <https://openreview.net/forum?id=PqvMRDCJT9t>.
- [20] Qinqing Zheng et al. “Guided Flows for Generative Modeling and Decision Making”. In: *arXiv preprint arXiv:2311.13443* (2023).
- [21] Yair Schiff et al. “Simple Guidance Mechanisms for Discrete Diffusion Models”. In: *The Thirteenth International Conference on Learning Representations*. 2025. URL: <https://openreview.net/forum?id=i5MrJ6g5G1>.
- [22] Yifei Shen et al. “Understanding and Improving Training-free Loss-based Diffusion Guidance”. In: *arXiv preprint arXiv:2403.12404* (2024).
- [23] Haotian Ye et al. “TFG: Unified Training-Free Guidance for Diffusion Models”. In: *The Thirty-eighth Annual Conference on Neural Information Processing Systems*. 2024. URL: <https://openreview.net/forum?id=N8YbGX98vc>.
- [24] Tero Karras et al. “Analyzing and Improving the Training Dynamics of Diffusion Models”. In: *Proc. CVPR*. 2024.
- [25] Anonymous. “Conditional Image Synthesis with Diffusion Models: A Survey”. In: *Submitted to Transactions on Machine Learning Research* (2024). Under review. URL: <https://openreview.net/forum?id=ewwNKwh6SK>.
- [26] Nikolas Adaloglou and Tim Kaiser. “An overview of classifier-free guidance for diffusion models”. In: *theaisummer.com* (2024). URL: <https://theaisummer.com/classifier-free-guidance>.

- [27] Xi Wang et al. “Analysis of Classifier-Free Guidance Weight Schedulers”. In: *arXiv preprint arXiv:2404.13040* (2024).
- [28] Mengfei Xia et al. “Rectified Diffusion Guidance for Conditional Generation”. In: *arXiv preprint arXiv:2410.18737* (2024).
- [29] Martin Heusel et al. In: *Advances in Neural Information Processing Systems*. 2017. URL: https://proceedings.neurips.cc/paper_files/paper/2017/file/8a1d694707eb0fefe65871369074926d-Paper.pdf.
- [30] George Stein et al. “Exposing flaws of generative model evaluation metrics and their unfair treatment of diffusion models”. In: *Thirty-seventh Conference on Neural Information Processing Systems*. 2023. URL: <https://openreview.net/forum?id=08zf7kT0oh>.
- [31] Felix Koulischer et al. “Dynamic Negative Guidance of Diffusion Models”. In: *The Thirteenth International Conference on Learning Representations*. 2025. URL: <https://openreview.net/forum?id=6p74UyAdLa>.
- [32] Mingyu Kim et al. “Training-Free Safe Denoisers for Safe Use of Diffusion Models”. In: *arXiv preprint arXiv:2502.08011* (2025).
- [33] Manuel Brack et al. “SEGA: Instructing Text-to-Image Models using Semantic Guidance”. In: *Thirty-seventh Conference on Neural Information Processing Systems*. 2023. URL: <https://openreview.net/forum?id=KIPAIy329j>.
- [34] Dazhong Shen et al. “Rethinking the Spatial Inconsistency in Classifier-Free Diffusion Guidance”. In: *2024 IEEE/CVF Conference on Computer Vision and Pattern Recognition (CVPR)*. 2024. DOI: 10.1109/CVPR52733.2024.00895.
- [35] Tim Kaiser, Nikolas Adaloglou, and Markus Kollmann. “The Unreasonable Effectiveness of Guidance for Diffusion Models”. In: *arXiv preprint arXiv:2411.10257* (2024).
- [36] Tiancheng Li et al. “Self-Guidance: Boosting Flow and Diffusion Generation on Their Own”. In: *arXiv preprint arXiv:2412.05827* (2024).
- [37] Nanye Ma et al. “Inference-Time Scaling for Diffusion Models beyond Scaling Denoising Steps”. In: *arXiv preprint arXiv:2501.09732* (2025).
- [38] Yingqing Guo et al. “Training-Free Guidance Beyond Differentiability: Scalable Path Steering with Tree Search in Diffusion and Flow Models”. In: *arXiv preprint arXiv:2502.11420* (2025).
- [39] Marta Skreta et al. “The Superposition of Diffusion Models Using the Itô Density Estimator”. In: *The Thirteenth International Conference on Learning Representations*. 2025. URL: <https://openreview.net/forum?id=2o58Mbqkd2>.
- [40] Rafal Karczewski, Markus Heinonen, and Vikas Garg. “Diffusion Models as Cartoonists: The Curious Case of High Density Regions”. In: *The Thirteenth International Conference on Learning Representations*. 2025. URL: <https://openreview.net/forum?id=RiS2cxpENN>.
- [41] Tuomas Kynkäänniemi et al. “Improved Precision and Recall Metric for Assessing Generative Models”. In: *Advances in Neural Information Processing Systems*. Vol. 32. 2019. URL: https://proceedings.neurips.cc/paper_files/paper/2019/file/0234c510bc6d908b28c70ff313743079-Paper.pdf.
- [42] Jia Deng et al. “ImageNet: A large-scale hierarchical image database”. In: *2009 IEEE Conference on Computer Vision and Pattern Recognition*. 2009. DOI: 10.1109/CVPR.2009.5206848.
- [43] Arwen Bradley and Preetum Nakkiran. “Classifier-Free Guidance is a Predictor-Corrector”. In: *NeurIPS 2024 Workshop on Mathematics of Modern Machine Learning*. 2024. URL: <https://openreview.net/forum?id=2dZswRE2sD>.
- [44] Muthu Chidambaram et al. “What does guidance do? A fine-grained analysis in a simple setting”. In: *The Thirty-eighth Annual Conference on Neural Information Processing Systems*. 2024. URL: <https://openreview.net/forum?id=AdS3H8SaPi>.
- [45] Sinho Chewi et al. “DDPM Score Matching and Distribution Learning”. In: *arXiv preprint arXiv:2504.05161* (2025).

A Theoretical shortcomings of CFG resolved by FBG

Despite being standardly used in practice, CFG remains vastly misunderstood [43, 44]. The common loose understanding of guidance is that to reinforce the conditioning signal of the models the aim is to sample from a λ -sharpened distribution, i.e. from $\tilde{p}(x|c) = p(x)p(c|x)^\lambda$. From this it is typical to derive $\nabla \log \tilde{p}(x|c)$ and obtain the standard linear combination of conditional and unconditional scores used in all variants of guidance [6, 7].

What it is often overlooked is that this mixing of the distribution is defined *locally*, at a specific noise level defined by t . By assuming an equivalent multiplicative mixing at every noise level, as for instance the case when using a constant guidance scale in CFG, the sampled marginals do not correspond to the predefined forward process. In essence the common misunderstanding is that the mixing operation commutes with the noising operation, i.e. that mixing the noise-free distributions and noising them is equivalent to first noising the distributions and then only mixing them, which is erroneous. In other words, in the case of a multiplicative mixture one can not simply mix the clean distributions, add a subscript t everywhere and expect these to sample from the desired marginals. When following the score functions defined using the CFG equation, one is not sampling from the intuitively sharpened data distribution $\tilde{p}(x|c) = p(x)p(c|x)^\lambda$ [43, 44].

To sample the γ -sharpened conditional distribution in the clean image space using the forward process defined by the diffusion kernel $k(\mathbf{x}_s, \mathbf{x}_t)$ the marginals at timestep t should correspond to:

$$\begin{aligned} \tilde{p}_t(\mathbf{x}_t|c) &= \int d\mathbf{x}_0 \tilde{p}_0(\mathbf{x}_0|c) k(\mathbf{x}_0, \mathbf{x}_t) \\ &= \int d\mathbf{x}_0 p_{\theta,0}(\mathbf{x}_0|c)^\lambda p_{\theta,0}(\mathbf{x}_0)^{1-\lambda} k(\mathbf{x}_0, \mathbf{x}_t) \end{aligned} \quad (12)$$

However, when sampling using the score function defined by CFG we are implicitly assuming that the marginals at timestep t keep the mixing property:

$$\begin{aligned} \tilde{p}_{t,CFG}(\mathbf{x}_t|c) &= p_{\theta,t}(\mathbf{x}_t|c)^\lambda p_{\theta,t}(\mathbf{x}_t)^{1-\lambda} \\ &= \left(\int d\mathbf{x}_0 \tilde{p}_0(\mathbf{x}_0|c) k(\mathbf{x}_0, \mathbf{x}_t) \right)^\lambda \left(\int d\mathbf{x}_0 \tilde{p}_0(\mathbf{x}_0) k(\mathbf{x}_0, \mathbf{x}_t) \right)^{1-\lambda} \end{aligned} \quad (13)$$

These two expressions are not equal and can in fact differ significantly especially at higher noise levels, at which the overlap between $p_t(x|c)$ and $p_t(x)$ is significant as the information of the underlying distributions has been nearly entirely removed, i.e. both distributions start to resemble gaussian distributions. This implies that the trajectories sampled under CFG simply do not correspond to the predefined forward process, especially at high noise levels. The main consequence of this is that sampling using CFG can be very misleading.

Mathematically the non-commutability of the mixing and noising operations in the case of CFG is due to the non-commutability of the multiplication and convolution operations. The proposed *additive* error at the heart of our FBG approach does not suffer from the same flaws. Thanks to the commutability of the addition and the convolution, the mixing and noising operations become interchangeable. This implies that when using the scores provided by Feedback guidance the predefined distribution is retrieved⁸.

Resolving this issue is not the main purpose of this work, which is why we for instance propose combining FBG with other guidance scheme such as CFG[7] or LIG[9]. Nonetheless, we believe this to be an insightful discussion worth mentioning and exploring.

B Posterior likelihood estimation

The estimation of the posterior likelihood is central to the proposed Feedback Guidance. Multiple approaches in the literature provide ways of estimating such densities [31, 39, 40, 45]. Seeing the similarities of the present work with the Dynamic Negative Guidance (DNG) approach, we keep the same notation [31]. For an intuitive explanation of the estimation, we refer the reader to the afore mentioned paper. The continuous limit is then derived in B.1. The key hyperparameters introduced in the main body are described in more detail in B.2.

⁸At least in the case that an exact posterior is available and that the to-be-sampled distribution is valid, i.e. satisfies positivity constraints.

B.1 Continuous limit

In this section, we derive the continuous-time limit of the posterior approximation used in Feedback Guidance (FBG). To this end, it suffices to consider the posterior update under the guided prediction: $\mathbf{x}_{t-1} = \boldsymbol{\mu}(\mathbf{x}_t) + \lambda(\boldsymbol{\mu}(\mathbf{x}_t|c) - \boldsymbol{\mu}(\mathbf{x}_t)) + \sigma_{t-1|t}\boldsymbol{\epsilon}$ with $\boldsymbol{\epsilon} \sim \mathcal{N}(0, \mathbf{I})$. This results in:

$$\begin{aligned}
\log p(c|\mathbf{x}_{t-1}) &= \log p_t(c|\mathbf{x}_t) - \frac{1}{2\sigma_{t-1|t}^2} (\|\mathbf{x}_{t-1} - \boldsymbol{\mu}(\mathbf{x}_t|c)\|^2 - \|\mathbf{x}_{t-1} - \boldsymbol{\mu}(\mathbf{x}_t)\|^2) \\
&= \log p_t(c|\mathbf{x}_t) - \frac{1}{2\sigma_{t-1|t}^2} (\|\boldsymbol{\mu}(\mathbf{x}_t) + \lambda(\mathbf{x}_t, t)(\boldsymbol{\mu}(\mathbf{x}_t|c) - \boldsymbol{\mu}(\mathbf{x}_t)) + \sigma_{t-1|t}\boldsymbol{\epsilon} - \boldsymbol{\mu}(\mathbf{x}_t|c)\|^2 \\
&\quad - \|\boldsymbol{\mu}(\mathbf{x}_t) + \lambda(\mathbf{x}_t, t)(\boldsymbol{\mu}(\mathbf{x}_t|c) - \boldsymbol{\mu}(\mathbf{x}_t)) + \sigma_{t-1|t}\boldsymbol{\epsilon} - \boldsymbol{\mu}(\mathbf{x}_t)\|^2) \\
&= \log p_t(c|\mathbf{x}_t) - \frac{\tau}{2\sigma_{t-1|t}^2} (\|(\lambda(\mathbf{x}_t, t) - 1)(\boldsymbol{\mu}(\mathbf{x}_t|c) - \boldsymbol{\mu}(\mathbf{x}_t)) + \sigma_{t-1|t}\boldsymbol{\epsilon}\|^2 \\
&\quad - \|\lambda(\mathbf{x}_t, t)(\boldsymbol{\mu}(\mathbf{x}_t|c) - \boldsymbol{\mu}(\mathbf{x}_t)) + \sigma_{t-1|t}\boldsymbol{\epsilon}\|^2) \\
&= \log p_t(c|\mathbf{x}_t) - \frac{\tau}{2\sigma_{t-1|t}^2} ((1 - 2\lambda(\mathbf{x}_t, t))\|\boldsymbol{\mu}(\mathbf{x}_t|c) - \boldsymbol{\mu}(\mathbf{x}_t)\|^2 + 2\sigma_{t-1|t}\boldsymbol{\epsilon} \cdot (\boldsymbol{\mu}(\mathbf{x}_t|c) - \boldsymbol{\mu}(\mathbf{x}_t)))
\end{aligned} \tag{14}$$

The term added to the log posterior likelihood can be decomposed into two separate contributions. The first corresponds to a deterministic measure, evaluating how much the conditional and unconditional predictions differ $\|\boldsymbol{\mu}(\mathbf{x}_t) - \boldsymbol{\mu}(\mathbf{x}_t|c)\|^2$, while the second is a stochastic term that measures the overlap between this difference and the added stochastic noise. The former measures how much on average the predictions differ, while the latter measures if by chance the stochastic process has favored one over the other.

Using this understanding, a continuous form of the equations is recognisable. For this one has to realise that in the continuous case the backward and forward transition kernels become of equal variance, i.e. $\lim_{dt \rightarrow 0} \sigma_{t-dt|t}^2 = \sigma_{t|t-dt}^2$. Therefore up to first order one can approximate that $\sigma_{t-dt|t}^2 \approx \sigma_{t|t-dt}^2 = \sigma_t^2 - \sigma_{t-1}^2 = d\sigma_t^2/dt = 2\sigma_t\dot{\sigma}_t$. This results in the following continuous integral:

$$\log p(c|\mathbf{x}_t) = \int_t^T \frac{\tau}{4\sigma_s\dot{\sigma}_s} (2\lambda(\mathbf{x}_s, s) - 1) \|\boldsymbol{\mu}(\mathbf{x}_s|c) - \boldsymbol{\mu}(\mathbf{x}_s)\|^2 ds + 2 \int_t^T \sqrt{2\sigma_s\dot{\sigma}_s} (\boldsymbol{\mu}(\mathbf{x}_s|c) - \boldsymbol{\mu}(\mathbf{x}_s)) \cdot d\mathbf{W} \tag{15}$$

The first integral is a path integral, capturing the cumulative deterministic contribution over the diffusion path. The second integral is a stochastic Itô integral over the Wiener process $d\mathbf{W}$, capturing how the stochastic noises influence over the posterior likelihood.

B.2 Understanding the hyperparameters for the posterior estimation

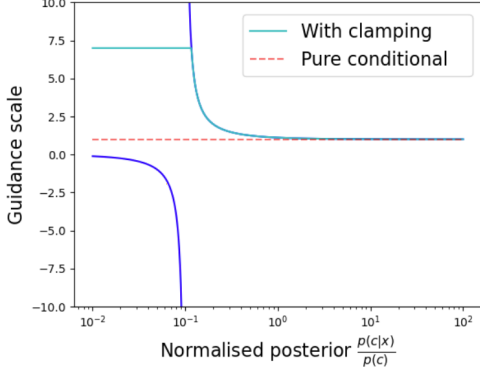
The hyperparameters π , τ , and δ play a central role in Feedback Guidance (FBG), but their interdependence and abstract nature can hinder accessibility and ease of tuning. To mitigate this, we propose a reparametrization of the temperature and offset parameters, τ and δ , in terms of the mixing parameter π and two new hyperparameters— t_0 and t_1 —which correspond to normalized diffusion times ($t = 0$ denotes clean data; $t = 1$ denotes fully noised data).

Understanding the influence of these parameters requires analyzing how the posterior, and thereby the guidance scale $\lambda(\mathbf{x}, t)$, depends on them.

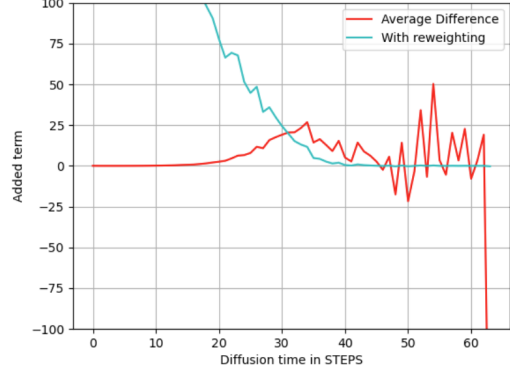
Effect of mixing parameter π

The mixing parameter π controls the point at which the guidance scale $\lambda(\mathbf{x}, t)$ becomes large. Specifically, λ diverges when $p(c|\mathbf{x}_t) \approx 1 - \pi$. Thus, adjusting π shifts the asymptotic region of the guidance curve. In Fig. 7a, we illustrate this behavior by plotting the posterior values at which $\lambda = 3$ for various values of π . As π increases, stronger confidence (i.e., lower posterior values) is required to activate a given level of guidance. Intuitively, when $\pi \rightarrow 1$, the conditional model closely approximates the true posterior, and additional guidance is only necessary when uncertainty is high.

Motivation for Offset parameter δ

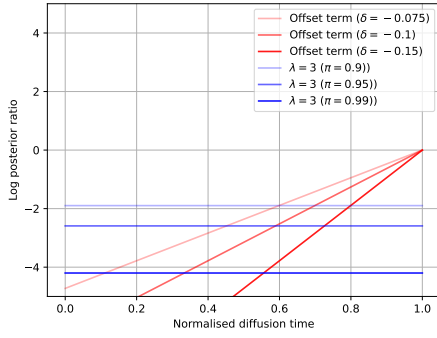


(a) Guidance as function of posterior

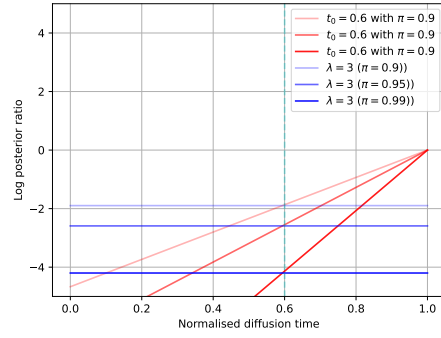


(b) Average term added at each timestep

Figure 6: In (a) the guidance scale is plotted as a function of the posterior. Here it is important to note that we argue that in practice the negative part of the curve is never reached as in a continuous process the crossing of the asymptote would result in an infinite amount of guidance. In practice to avoid this happening upon discretisation a maximal guidance value can be set, as shown in the light blue line. In (b) an average of the added term is shown. The red line corresponds to the euclidean difference, whereas the light-blue line includes the reweighting by the transition kernel variance $\sigma_{t-1|t}^2$



(a) π , δ dependence



(b) π , t_0 dependence

Figure 7: Illustration of the interplay between π and δ in (a) and t_0 in (b). When specifying t_0 the value of δ is chosen such that the intersection of the red and blue lines is located at t_0 .

In the early diffusion steps, when noise dominates, the trajectory of the generated sample is best approximated by the conditional model itself, i.e., $\mathbf{x}_{t-1} \approx \boldsymbol{\mu}_{t,\theta}(\mathbf{x}_t|c)$. Neglecting stochasticity, the posterior update simplifies to:

$$\begin{aligned} \log p_t(c|\mathbf{x}_t) &= \log p_{t+1}(c|\mathbf{x}_{t+1}) - \frac{1}{2\sigma_{t|t+1}^2} (\|\mathbf{x}_t - \boldsymbol{\mu}_{t,\theta}(\mathbf{x}_{t+1}|c)\|^2 - \|\mathbf{x}_t - \boldsymbol{\mu}_{t,\theta}(\mathbf{x}_{t+1})\|^2) \\ &\approx \log p_{t+1}(c|\mathbf{x}_{t+1}) + \frac{1}{2\sigma_{t|t+1}^2} \|\mathbf{x}_t - \boldsymbol{\mu}_{t,\theta}(\mathbf{x}_{t+1})\|^2 \end{aligned} \quad (16)$$

This leads to a monotonically increasing posterior, which artificially inflates model confidence and suppresses guidance activation. To address this, we introduce a linear transformation with an offset δ :

$$\log p_t(c|\mathbf{x}_t) = \log p_{t+1}(c|\mathbf{x}_{t+1}) - \frac{\tau}{2\sigma_{t|t+1}^2} (\|\mathbf{x}_t - \boldsymbol{\mu}_{t,\theta}(\mathbf{x}_{t+1}|c)\|^2 - \|\mathbf{x}_t - \boldsymbol{\mu}_{t,\theta}(\mathbf{x}_{t+1})\|^2) - \delta \quad (17)$$

This correction is especially important in the early diffusion regime, where the signal-to-noise ratio is low and the posterior estimate is dominated by the offset. Under the EDM scheduler, where $\sigma_t^2 \in [0.002, 80]$, the transition variance $\sigma_{t-1|t}^2 = \sigma_t^2(1 - \sigma_{t-1}^2/\sigma_t^2)$ spans an extremely wide range, exacerbating this effect.

To make this more interpretable, we define δ in terms of π and a new hyperparameter t_0 , defined as the timestep at which the guidance scale reaches a reference value $\lambda_{\text{ref}} = 3$ under a purely linear model. This yields:

$$\delta = \frac{1}{N_{\text{steps}}(1 - t_0)} \log \left((1 - \pi) \cdot \frac{\lambda_{\text{ref}}}{\lambda_{\text{ref}} - 1} \right) \quad (18)$$

Reparameterising the temperature τ

We now reparametrize τ using t_0 and t_1 , where t_1 represents the timestep at which the additive Euclidean term matches the magnitude of the offset δ . To estimate this, we compute the average contribution Δ of the Euclidean difference across sampled trajectories (see Fig. 6b). For the EDM2-XS model, we find $\Delta \approx 10$ around $t = 0.5$.

This gives:

$$\tau = \frac{2\tilde{\sigma}_{t_0}}{\Delta} \cdot \delta \quad (19)$$

While Δ is not a tunable hyperparameter, using it improves interpretability: t_1 now corresponds to the point at which guidance begins to decrease, marking the transition to effective conditional denoising.

Summary

By reparametrizing the abstract hyperparameters τ and δ in terms of normalized diffusion times t_0 and t_1 , we provide a more intuitive interface for tuning Feedback Guidance. This improves both usability and interpretability, which we consider essential for practical deployment.

C Stochastic sampling for Variance Exploding Diffusion Models

It is well known the forward process can be freely chosen. Two very standard cases are those of a *Variance Preserving* (VP) and that of a *Variance Exploding* (VE) forward process.

In the VP case, the information is progressively destroyed by both downscaling the features by a factor $\sqrt{\alpha_t}$ and adding normal noise with standard deviation $\sqrt{1 - \alpha_t}$, i.e. $\mathbf{x}_{t+1} = \sqrt{\alpha_t}\mathbf{x}_t + \sqrt{1 - \alpha_t}\boldsymbol{\epsilon}$ with $\boldsymbol{\epsilon} \sim \mathcal{N}(\mathbf{0}, \mathbf{I})$. This forward transition can alternatively be described by $\mathbf{x}_{t+1} \sim q(\mathbf{x}_{t+1}|\mathbf{x}_t)$ with $q(\mathbf{x}_{t+1}|\mathbf{x}_t) = \mathcal{N}(\sqrt{\alpha_t}\mathbf{x}_t, (1 - \alpha_t)\mathbf{I})$. Thanks to a nice property of the Gaussian function, this Markov chain can be reparameterised as $\mathbf{x}_{t+1} \sim q(\mathbf{x}_{t+1}|\mathbf{x}_0)$ with $q(\mathbf{x}_{t+1}|\mathbf{x}_0) = \mathcal{N}(\sqrt{\bar{\alpha}_t}\mathbf{x}_0, (1 - \bar{\alpha}_t)\mathbf{I})$ and $\bar{\alpha}_t = \prod_{s=0}^t \alpha_s$. This forward process can then be inverted according to $\mathbf{x}_{t-1} \sim p(\mathbf{x}_{t-1}|\mathbf{x}_t)$ with $p(\mathbf{x}_{t-1}|\mathbf{x}_t) = \mathcal{N}(\boldsymbol{\mu}_t, \tilde{\sigma}_t^2\mathbf{I})$. In this case, it is well known that $\boldsymbol{\mu} = \frac{1}{\sqrt{\alpha_t}}(\mathbf{x}_t - \frac{1 - \alpha_t}{\sqrt{1 - \bar{\alpha}_t}}\boldsymbol{\epsilon}_t)$ and $\tilde{\sigma}_t = \frac{1 - \bar{\alpha}_{t-1}}{1 - \bar{\alpha}_t}\beta_t$.

The case of VE is far less often described using the discrete markov chain framework, which is why we think it wise to derive the precise shape of $\mathbf{x}_{t-1} \sim p(\mathbf{x}_{t-1}|\mathbf{x}_t)$ with $p(\mathbf{x}_{t-1}|\mathbf{x}_t) = \mathcal{N}(\boldsymbol{\mu}_t, \tilde{\sigma}_t^2\mathbf{I})$. In the VE case, the forward process simply consists of adding gaussian noise of increasing scale $\mathbf{x}_{t+1} = \mathbf{x}_t + \sqrt{\sigma_{t+1}^2 - \sigma_t^2}\boldsymbol{\epsilon}$ with $\boldsymbol{\epsilon} \sim \mathcal{N}(\mathbf{0}, \mathbf{I})$. Similarly to the VP case, the previous process can be reparameterise $\mathbf{x}_{t+1} \sim q(\mathbf{x}_{t+1}|\mathbf{x}_0)$ with $q(\mathbf{x}_{t+1}|\mathbf{x}_0) = \mathcal{N}(\mathbf{x}_0, \sigma_{t|0}^2\mathbf{I})$ and $\sigma_{t|0}^2 = \sum_{s=0}^t \sigma_s^2$. To obtain the form of $p(\mathbf{x}_{t-1}|\mathbf{x}_t) = \mathcal{N}(\boldsymbol{\mu}_t\sigma_{t-1|t}^2\mathbf{I})$ we need to obtain $q(\mathbf{x}_{t-1}|\mathbf{x}_t, \mathbf{x}_0)$ which is obtainable thanks to the conditioning on \mathbf{x}_0 . One finds:

$$\begin{aligned}
p(\mathbf{x}_{t-1}|\mathbf{x}_t, \mathbf{x}_0) &= q(\mathbf{x}_t|\mathbf{x}_{t-1}, \mathbf{x}_0) \frac{q(\mathbf{x}_{t-1}|\mathbf{x}_0)}{q(\mathbf{x}_t|\mathbf{x}_0)} \\
&\propto \exp\left(-\frac{1}{2}\left[\frac{\|\mathbf{x}_t - \mathbf{x}_{t-1}\|^2}{\sigma_t^2 - \sigma_{t-1}^2} + \frac{\|\mathbf{x}_{t-1} - \mathbf{x}_0\|^2}{\sigma_{t-1}^2} + \frac{\|\mathbf{x}_t - \mathbf{x}_0\|^2}{\sigma_t^2}\right]\right) \\
&= \exp\left(-\frac{1}{2}\left[\left(\frac{1}{\sigma_t^2 - \sigma_{t-1}^2} + \frac{1}{\sigma_{t-1}^2}\right)\|\mathbf{x}_{t-1}\|^2\right.\right. \\
&\quad \left.\left.- 2\left(\frac{1}{\sigma_t^2 - \sigma_{t-1}^2}\mathbf{x}_t + \frac{1}{\sigma_{t-1}^2}\mathbf{x}_0\right)\mathbf{x}_{t-1} + c(\mathbf{x}_t, \mathbf{x}_0)\right]\right) \\
&\propto \exp\left(-\frac{\|\mathbf{x}_{t-1} - \boldsymbol{\mu}_t\|^2}{2\sigma_{t-1|t}^2}\right)
\end{aligned} \tag{20}$$

Rewriting the clean data points \mathbf{x}_0 using the ground truth noise $\boldsymbol{\epsilon}_t$ through $\mathbf{x}_0 = \mathbf{x}_t - \sigma_t \boldsymbol{\epsilon}_t$. This is done because this is precisely how our denoising network will be parametrized. Using this, one recognizes:

$$\begin{aligned}
\sigma_{t-1|t}^2 &= (\sigma_t^2 - \sigma_{t-1}^2) \frac{\sigma_{t-1}^2}{\sigma_t^2} \\
\boldsymbol{\mu}_t &= \mathbf{x}_t - \left(1 - \frac{\sigma_{t-1}^2}{\sigma_t^2}\right) \sigma_t \boldsymbol{\epsilon}_t
\end{aligned} \tag{21}$$

Or alternatively using the score function, i.e. $\boldsymbol{\epsilon}_t = \sigma_t \nabla_{\mathbf{x}} \log p_t$, we have:

$$\boldsymbol{\mu}_t = \mathbf{x}_t - (\sigma_t^2 - \sigma_{t-1}^2) \nabla_{\mathbf{x}} \log p_t \tag{22}$$

Or equivalently, the very intuitive equation:

$$\nabla_{\mathbf{x}} \log p_t = \frac{\mathbf{x}_t - \boldsymbol{\mu}_t}{\sigma_t^2 - \sigma_{t-1}^2} \tag{23}$$

D Additional results and ablations

In this appendix all the additional ablations and obtained results are provided and described in more detail.

First and foremost the hyperparameters of the three guidance schemes that minimize the FID or $\text{FD}_{\text{DinoV2}}$ are provided in Table 2.

For CFG a sweep over the guidance scale is performed at a resolution of $\lambda = 0.125$.

For LIG a joint sweep over the guidance scale and the starting point of guidance is done. The sweep over the guidance scale is performed at a resolution of $\lambda = 0.25$ and the starting point σ_{\max} is chosen at the discretised step values. The influence of the end point of guidance is not analysed, instead a low value of $\sigma_{\min} = 0.28$ is chosen. As highlighted in the work in which the method is introduced, increasing σ_{\min} leaves the FID unaltered and is simply beneficial from a computational point of view [9].

For FBG a joint sweep over t_0 and $t_0 - t_1$ is performed defined as the normalised diffusion times corresponding with the discrete step values. For instance in the case of stochastic sampling where 64 sampling steps are used we perform a sweep at a resolution of $t_0 = 1/64 \simeq 0.0156$. We prefer to define t_1 as a function of t_0 , as their difference gives an estimate for how large the guidance interval is. This is then repeated for three values of $\pi = 0.999, 0.9999, 0.99999$. These values were chosen after a preliminary finetuning by hand. We find that although the guidance profiles do differ slightly between different choices of π , mainly being sharper as π increases, the optimal FID/ $\text{FD}_{\text{DinoV2}}$ remain very similar. Due to this we choose to focus our limited resources on a proper ablation at a fixed value of $\pi = 0.9999$. To illustrate the weak dependence of FBG on values of π a sweep is performed using the optimal values for t_0 and t_1 given in table 2. The results are shown in Fig. 9, where it can be seen that both FID and $\text{FD}_{\text{DinoV2}}$ values remain fairly constant over a wide range of π -values.

It should also be noted that at some point in the research process we tried adding a late start to the offset parameter, i.e. to set $\delta = 0$ for $t > t_{\text{start-offset}}$, and slightly modify the way we parameterise δ as a function of t_0 such that its interpretation remains true. This however did not significantly

Guidance scheme	CFG[7]	LIG [9]			FBG _{pure} (ours)			FBG _{LIG} (ours)	
	λ	λ	σ_{\max}	σ_{\min}	π	σ_{t_0}	σ_{t_1}	λ	σ_{t_1}
Stoch. (FID)	1.4	2.8	1.6	0.15	0.999	1.10	0.56	1.4	4.64
PFODE (FID)	1.4	2.2	2.9	0.41	0.999	1.61	0.60	2.6	2.7
Stoch. (FD _{DinoV2})	2.1	2.9	6.8	0.48	0.999	4.07	1.29	2.6	2.34
PFODE (FD _{DinoV2})	2.3	2.8	16.6	0.80	0.999	6.46	1.17	1.6	1.61

Table 2: Optimal hyperparameters for different sampling approaches. To facilitate the comparison between the schemes we follow the nomenclature introduced of the EDM framework [5] and refer to the noise levels σ_{t_0} , σ_{t_1} instead of normalized diffusion times t_0 and t_1 for FBG. For FBG_{LIG} the unspecified parameters (π , t_0 , σ_{\max} and σ_{\min}) are left unaltered from the separately optimised methods.

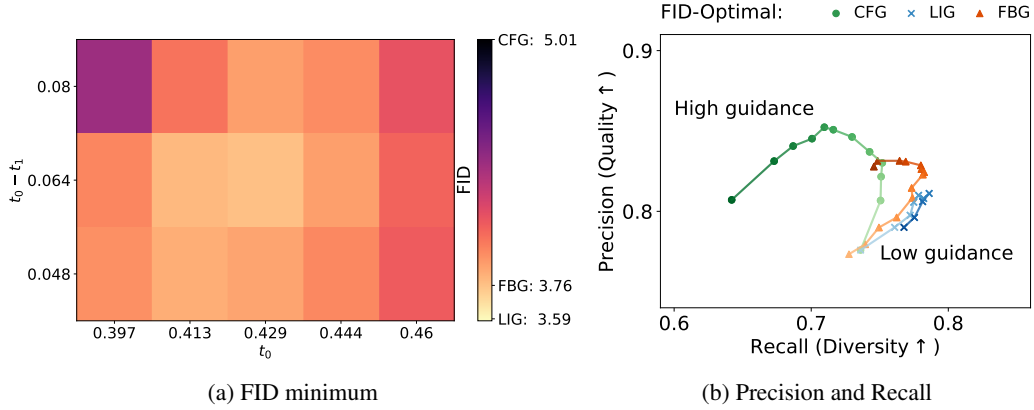


Figure 8: Grid search over the two hyperparameters t_0 and t_1 . The FID is shown calibrated within the best performing value using LIG and CFG.

modify the performance of the approach, so this research track was dropped to avoid any unnecessary convolutions. For all methods we find that the FD_{DinoV2}-optimal hyperparameter values result in a much higher amount of guidance than the FID-optimized values, hinting that the metrics are not sensitive to the same features [30]. This fact highlights that only providing one of the two metrics when benchmarking a new approach might not provide the full story.

Figure 8 is the corresponding figure to Fig. 3 in the main body, but for the FID-optimised stochastic sampling, rather than for FD_{DinoV2}.

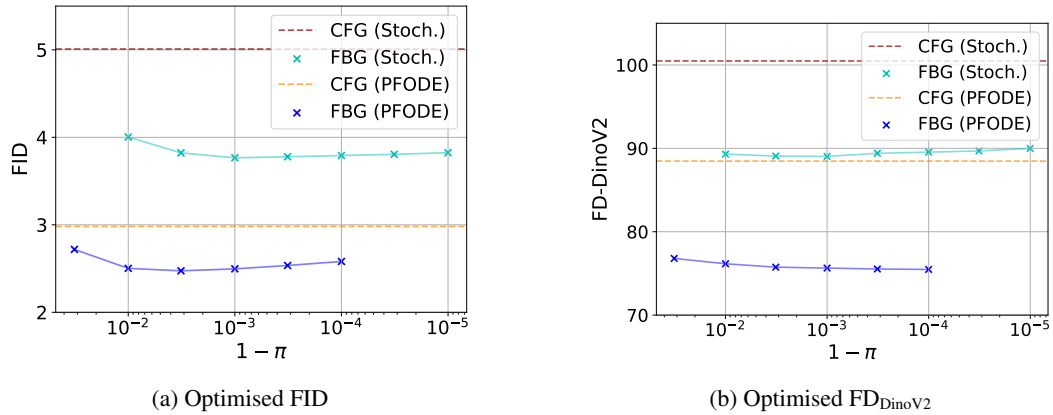


Figure 9: Illustration of the weak π dependence of FBG when parametrised using t_0 and t_1 . The sweep over π is performed at the optimal values for t_0 and t_1 given to in Table 2.

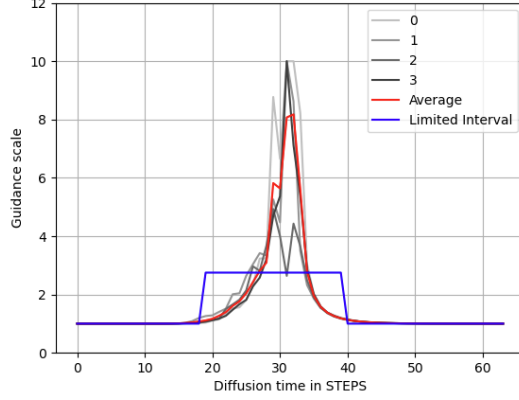


Figure 10: Comparing the guidance scale predicted by FBG and that of LIG in the FD_{DinoV2} optimized setting. Despite possessing similarities the two seem to operate in different regimes.

D.1 Combined guidance schemes

The proposed Feedback Guidance scheme can be easily combined with other preexisting guidance schemes such as Classifier-Free Guidance [7] or Limited Interval Guidance [9].

In the context of Text-To-Image we observe that adding a base level of CFG can help to retrieve the low frequency features of an image, such as sharp colors, without drastically harming the diversity. In the context of Imagenet generation using EDM2-XS, we find that using FBG_{LIG} which combines FBG_{pure} with LIG, is optimal. Preliminary results indicate that joint methods easily outperform their parts. That such results are obtained in this context should not surprise the reader, both method despite having some similarities, behave very differently as illustrated in Fig. 10. To simplify hyperparameter tuning of FBG_{LIG} , we suggest to use the optimal time interval parameters of LIG with slightly less guidance and to slightly reduce $t_1 - t_0$ for FBG_{pure} . In essence, both of these subtle changes are responsible for less guidance of the respective schemes, which makes sense as the two are later on combined.

The optimal values for the sweep over λ_{LIG} and t_1 are given in Table 2. The other parameters are chosen the same as the separately optimized methods. We do not exclude the possibility that a full grid-search over the entire joint hyperparameter space might yield better trade-offs between the two guidance schemes.

An advantage of the error assumption model proposed is that it allows for a very flexible view of guidance. For instance, for the FBG_{CFG} approach in fact simply corresponds to assuming that the true conditional distribution can be rewritten as:

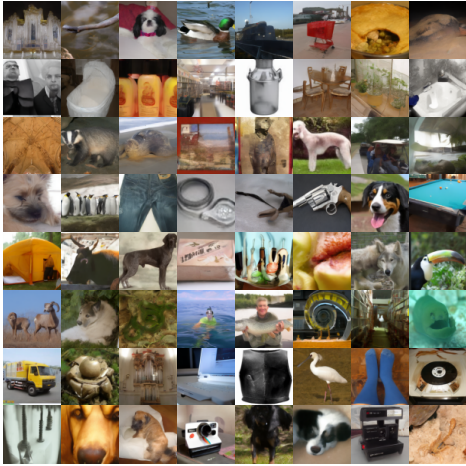
$$p_t(\mathbf{x}_t|c) = \frac{1}{\pi} (p_{t,\theta}(\mathbf{x}_t|c) - (1 - \pi)p_\theta(\mathbf{x}_t)) \frac{p_{t,\theta}(\mathbf{x}_t|c)^{\lambda-1}}{p_{t,\theta}(\mathbf{x}_t)^{\lambda-1}} \quad (24)$$

This implies that the learned distribution satisfies the following algebraic equation:

$$p_{t,\theta}(\mathbf{x}_t|c)^\lambda - (1 - \pi)p_{t,\theta}(\mathbf{x}_t|c)^{\lambda-1}p_t(\mathbf{x}_t) = \pi p_t(\mathbf{x}_t|c)p_t(\mathbf{x}_t)^{\lambda-1} \quad (25)$$

Similarly, FBG_{LIG} assumes the same form of error with as only distinction that λ becomes a time dependent function that is equal to one outside the guidance interval specified by σ_{min} and σ_{max} .

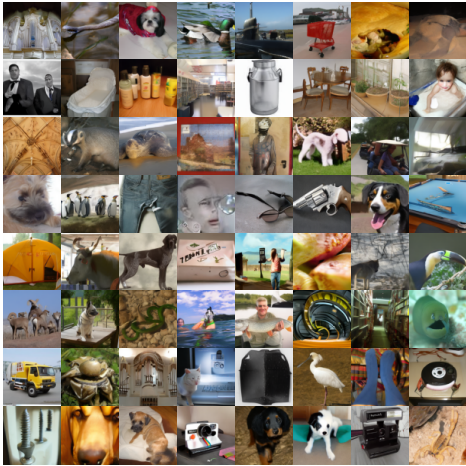
D.2 Illustrative samples (EDM2-XS)



(a) FID-optimal CFG



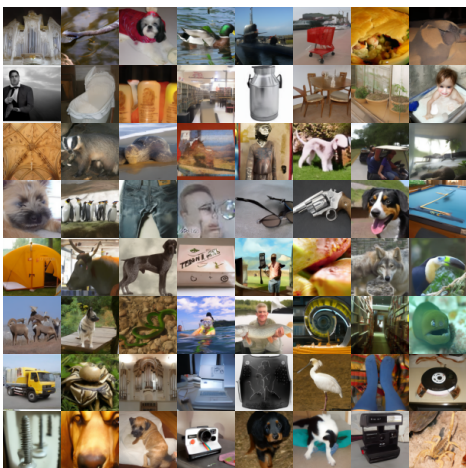
(b) FD_{DinoV2}-optimal CFG



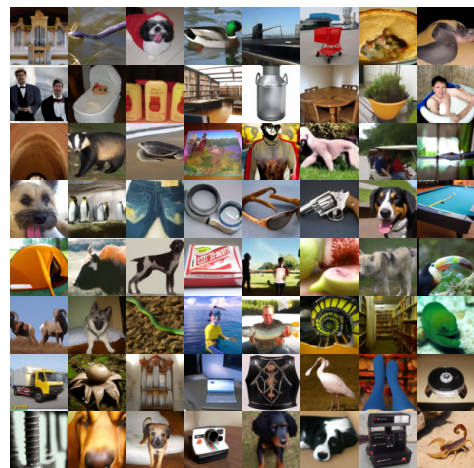
(c) FID-optimal LIG



(d) FD_{DinoV2}-optimal LIG



(e) FID-optimal FBG (ours)



(f) FD_{DinoV2}-optimal FBG (ours)

Figure 11: Grids containing samples generated using the different guidance schemes CFG, LIG and FBG (ours). Results displayed under the same seed and when the hyperparameters are optimised for both FID and FD_{DinoV2}-optimal performance.

Difficulty	Category	Prompt
Memorized	Artwork	The starry night by Van Gogh
Memorized	Brand	The Nike brand logo
Memorized	Location	A photo of the Taj Mahal in India
Basic	Animal	An orange cat sitting on a couch
Basic	Food	A pizza slice on a white plate
Basic	Nature	A bird nest with three blue eggs
Intermediate	Animal	A dolphin jumping through a hoop made of fire
Intermediate	Food	A floating sushi platter arranged in the shape of a koi fish, hovering over a pond
Intermediate	Nature	A desert landscape with an abandoned train half-buried in the sand
Very hard	Animal	A parrot with steampunk goggles flying through a thunderstorm above a 19th-century shipwreck, in dramatic oil painting style
Very hard	Food	A glass teapot filled with herbal tea where each herb leaf is shaped like a different mythical creature, photographed on white marble
Very hard	Nature	A city built inside a giant canyon where each layer of rock houses a different civilization, all lit by bioluminescent flora

Table 3: Example prompts from the dataset, sorted by difficulty and category

E Prompt dataset

To analyse the sensitivity of our dynamic guidance scale to the complexity of the given prompts, a small scale prompt dataset is introduced. It contains 60 prompts of 4 difficulty levels: memorized, basic, intermediate and hard. Each complexity level is divided into 3 categories/topics containing 5 prompts each.

For the memorized prompts we use: well known artworks, brands and locations.

For the other three we use: animal, food and nature images.

The prompts themselves are generated using ChatGPT and further minimally modified to make the prompt easier to verify. The main difference between *basic* and *intermediate* prompts is that the latter contain highly unlikely combinations (such as "A giraffe playing basketball on rollerskates") that the model has most likely not seen (or only rarely) as such in the training data. The main difference between *intermediate* and *hard* prompts is mainly the amount of details contained in the prompt. The more details such as colours, numbers or different elements are added, the more unlikely it becomes that the conditional model will be to satisfy all prerequisites on its own.

The dataset is available in the official repository at this link. Examples of each difficulty level and each category are given in Table 3.

F Used resources

For the stochastic sampler all experiments are run using on a NVIDIA Tesla V100-SXM3-32GB GPU. Generating 50k images in batches of 64 using the EDM2-XS model [8, 24], as required for a valid FID benchmark [29, 30], takes 7h30 on such a node. For the 2nd-order Heun sampler of the PFODE [5, 24] a NVIDIA GeForce RTX 4090 GPU is used. Generating 50k images in batches of 64 using the EDM2-XS model [8, 24], as required for a valid FID benchmark [29, 30], takes 8h on such a node. For the T2I results using Stable diffusion 2[18], we rely on a NVIDIA GeForce GTX 1080 Ti GPU. These can be used, because the experiments performed only require the generation of around 2k images per hyperparameter setting, which takes around 6h on such a node.

NeurIPS Paper Checklist

1. Claims

Question: Do the main claims made in the abstract and introduction accurately reflect the paper's contributions and scope?

Answer: [Yes]

Justification: As discussed in the work, our approach is the first theoretically grounded state- and time-dependent guidance scale. The obtained trajectory specific guidance scale exhibits a behaviour similar to the ad-hoc proposed Limited Interval Guidance. When compared to CFG and LIG using the generated samples and robust metrics we find that our approach outperforms CFG and performs on par with the state of the art approach of LIG. It is our firm belief that FBG and its state- and time-dependent guidance scale that takes into account how good the model is at denoising the current state is not only highly novel but also promising.

2. Limitations

Question: Does the paper discuss the limitations of the work performed by the authors?

Answer: [Yes]

Justification: The paper contains a limitation section which provides a fair and honest evaluation of the proposed work.

3. Theory assumptions and proofs

Question: For each theoretical result, does the paper provide the full set of assumptions and a complete (and correct) proof?

Answer: [Yes]

Justification: The theoretical introduction of the additive error model and the resulting Feedback Guidance scheme is central to this work and therefore derived in detail.

4. Experimental result reproducibility

Question: Does the paper fully disclose all the information needed to reproduce the main experimental results of the paper to the extent that it affects the main claims and/or conclusions of the paper (regardless of whether the code and data are provided or not)?

Answer: [Yes]

Justification: A pseudocode of Feedback Guidance is provided in the main body. The introduced hyperparameters are discussed in detail at the end of section 3.4 and further explained in Appendix B.2. The code as well as the small scale prompt dataset are made public at this link.

5. Open access to data and code

Question: Does the paper provide open access to the data and code, with sufficient instructions to faithfully reproduce the main experimental results, as described in supplemental material?

Answer: [Yes]

Justification: The method is thoroughly described and should be reproducible from the document. The data and code are publicly available at this link.

6. Experimental setting/details

Question: Does the paper specify all the training and test details (e.g., data splits, hyperparameters, how they were chosen, type of optimizer, etc.) necessary to understand the results?

Answer: [Yes]

Justification: As afore mentioned, the introduced hyperparameters are discussed in detail at the end of section 3.4 and further explained in Appendix B.2. optimized values are clearly given in table 2. The data and code are publicly available at this link.

7. Experiment statistical significance

Question: Does the paper report error bars suitably and correctly defined or other appropriate information about the statistical significance of the experiments?

Answer: [No]

Justification: Due to the expensiveness of the FID/FD_{DinoV2} metrics requiring 50k images per data point, only a single value is reported. To compare different approaches, it is more relevant to make sure that the approaches are evaluated on the same seeds, as this eliminates the possible bias caused by class imbalances during sampling.

8. Experiments compute resources

Question: For each experiment, does the paper provide sufficient information on the computer resources (type of compute workers, memory, time of execution) needed to reproduce the experiments?

Answer: [Yes]

Justification: This information is disclosed in Appendix F

9. Code of ethics

Question: Does the research conducted in the paper conform, in every respect, with the NeurIPS Code of Ethics <https://neurips.cc/public/EthicsGuidelines?>

Answer: [Yes]

Justification: The proposed work conforms in every respect with the NeurIPS Code of Ethics.

10. Broader impacts

Question: Does the paper discuss both potential positive societal impacts and negative societal impacts of the work performed?

Answer: [NA]

Justification: The paper presents a theoretical contribution to diffusion guidance techniques, focusing on foundational aspects without proposing a concrete application or system for deployment. As such, the work does not raise immediate concerns related to malicious use, fairness, privacy, or security. While future practical applications of improved diffusion methods may have societal implications, our contribution is abstract and methodological, without a direct path to societal impact at this stage.

11. Safeguards

Question: Does the paper describe safeguards that have been put in place for responsible release of data or models that have a high risk for misuse (e.g., pretrained language models, image generators, or scraped datasets)?

Answer: [NA]

Justification: This work is purely theoretical and does not involve the release of models, datasets, or other assets that carry a high risk for misuse. As such, no safeguards are necessary or applicable.

12. Licenses for existing assets

Question: Are the creators or original owners of assets (e.g., code, data, models), used in the paper, properly credited and are the license and terms of use explicitly mentioned and properly respected?

Answer: [NA]

Justification: The paper does not use any external assets such as datasets, pretrained models, or third-party code. All theoretical derivations and results are original to the authors.

13. New assets

Question: Are new assets introduced in the paper well documented and is the documentation provided alongside the assets?

Answer: [Yes]

Justification: The data and code are publicly available at this link.

14. Crowdsourcing and research with human subjects

Question: For crowdsourcing experiments and research with human subjects, does the paper include the full text of instructions given to participants and screenshots, if applicable, as well as details about compensation (if any)?

Answer: [NA]

Justification: No human evaluations were performed.

15. **Institutional review board (IRB) approvals or equivalent for research with human subjects**

Question: Does the paper describe potential risks incurred by study participants, whether such risks were disclosed to the subjects, and whether Institutional Review Board (IRB) approvals (or an equivalent approval/review based on the requirements of your country or institution) were obtained?

Answer: [NA]

Justification: No human evaluations were performed.

16. **Declaration of LLM usage**

Question: Does the paper describe the usage of LLMs if it is an important, original, or non-standard component of the core methods in this research? Note that if the LLM is used only for writing, editing, or formatting purposes and does not impact the core methodology, scientific rigor, or originality of the research, declaration is not required.

Answer: [NA]

Justification: No large language models (LLMs) were used as a core methodological component in this work. Any use of LLMs was limited to standard writing assistance and did not affect the scientific content of the paper.